On the Performance of Narrow-Band Internet of Things (NB-IoT)

Yihenew Dagne Beyene, Riku Jäntti, Kalle Ruttik and Sassan Iraji
Department of Communications and Networking
School of Electrical Engineering
Aalto University, Finland
{yihenew.beyene, riku.jantti, kalle.ruttik, sassan.iraji}@aalto.fi

***Abstract*—Narrow-Band Internet of Things (NB-IoT) is 3GPP's cellular technology designed for narrow-band and Low-Power Wide Area Network (LPWN). NB-IoT provides deep indoor coverage for thousands of low-data-rate and low-powered devices. Coverage enhancement for devices in weak coverage condition is enabled by having signal repetitions over extended period of time in order to boost the signal quality. Performance gain from repetitions of signals is limited by channel estimation quality. In this paper we analyze impact of channel coherence time on the uplink coverage. In addition to analytical performance bound and simulation results, we also present coverage performance results from practical measurements using a NB-IoT prototype. It is reported how the NB-IoT coverage improvement is limited by the channel estimation quality and coherence time of the channel.**

I. Introduction

The Internet of Things (IoT) is a new paradigm that has emerged in cellular networks. IoT applications are becoming essential parts of telecommunications industry. According to Ericsson [1], there are more than 16 billion connected devices worldwide. By 2021 the number will grow to nearly 28 billion connections 53% of which are Machine-to-Machine (M2M) devices and consumer electronics other than mobile phones, PCs, laptops and tablets. Cisco [2] predicts that the number of networked devices per capita will grow from 2.2 in 2015 to 3.4 in 2020. Traditionally, the key drivers in mobile network technology evolution were human-centric applications that needed high-speed internet access. However, IoT applications have different characteristics in terms of traffic pattern (eg. periodic, low data rate), latency requirement (eg. delay tolerant), deployment density.

There are a number of wireless technologies that have been developed in order to address different segments of IoT connectivity. Some of these technologies are short-range solutions such as Bluetooth Low Energy (BLE), ZigBee, WirelessHART, 6LoWPAN and Z-Wave. These technologies can be used to connect sensors and other IoT devices to a gateway within a coverage range of tens or hundreds of meters. The gateways are then connected to the internet via wired or wireless (eg. cellular) networks. Low Power Wide Area Network (LPWAN) technologies, on the other hand, allow devices to be connected directly to the Internet. This makes them ideal for connecting a large number of devices from a single access point. There are a number of LPWAN technologies that operate in license-exempt bands (eg. LoRa [3], SigFox [4], IEEE 802.11ah [5]) and licensed bands (eg. 3rd Generation Partnership Project (3GPP) standards such as Long Term Evolution (LTE) Cat-0 and LTE-Cat-M.

Recently, 3GPP has introduced a new technology called Narrow-Band Internet of Things (NB-IoT) in Release 13 of its specification [6]. It was motivated by the need for competitive solution for low data rate Machine-Type Communication (MTC) market. The following objectives were set when the study item was created [7].

- *Improved indoor coverage:* The new technology should enable connectivity for the devices that are located in the challenging indoor places such as in apartment basements. The aim is to offer a data rate of at least 160 bits per second in uplink and in downlink at extended coverage range of 20 dB compared to legacy GPRS systems.
- *Support for a massive number of low throughput devices:* A massive number of IoT devices that occasionally transmit small packets of data should be supported over small chunks of spectrum. The traffic model assumes 40 devices per home or 20 devices per person.
- *Low delay sensitivity:* The new technology aims at applications that have relaxed delay requirement.
- *Ultra low device cost:* IoT devices should be very cheep such that they can be deployed in mass or even in disposable manner.
- *Low device power consumption:* The battery life of IoT devices reaches up to 10 years with 5 Watt-hours battery capacity and 120 minutes for uplink reporting interval.
- *Optimized network architecture:* Various enhancements of the network architecture are targeted towards better security and relaxed packet delay budget for small data access.

We have developed NB-IoT testbed according to the latest specifications [8], [9], [10]. The testbed integrates all possible error sources and gives indications how well the designed specification meets the coverage targets. Through simulations and testbed measurement results we report how the NB-IoT coverage improvement is limited by the channel estimation quality and coherence time of the channel.

A single NB-IoT carrier spans bandwidth of 180 kHz in uplink

978-1-5090-4183-1/17/$31.00 ©2017 IEEE

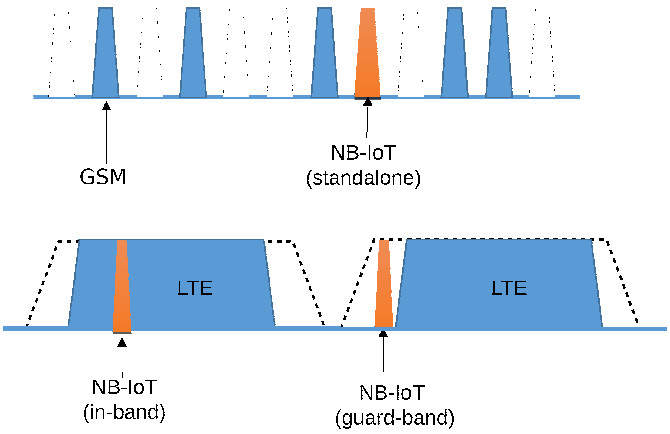

Fig. 1. NB-IoT Deployment Options.

and 180 kHz in downlink with Frequency Division Duplexing (FDD) [8]. This is equivalent to one Physical Resource Block (PRB) in LTE. Since NB-IoT requires narrow bandwidth, it can effectively use small chunks of re-farmed spectrum, for example, from GSM band or within existing LTE carrier. The NB-IoT standard defines three modes of operation as shown in Fig. 1. As in LTE, Orthogonal Frequency Division Multiplexing (OFDM) with 15 kHz sub-carrier spacing is used in downlink. On the other hand, in uplink both single-tone and multi-tone operations are supported. For single-tone operation, 3.75 kHz and 15 kHz sub-carrier spacing are supported. Multi-tone uplink transmission is according to Single-Carrier Frequency Division Multiple Access (SC-FDMA) with 15 kHz sub-carrier spacing.

NB-IoT supports repetition of signals in order to boost the signal power for low-powered devices that are in extreme coverage condition. The number of repetitions depends on the coverage enhancement level required by a User Equipment (UE) [9]. Up to 2048 and 128 repetitions are supported for downlink and uplink data transmissions respectively suggesting that data should be decoded even when the signal power is much smaller than the noise power. The decoding performance of coherent receivers is highly dependent on the channel estimation quality which limits the gain from having signal repetition. In NB-IoT, known reference pilot symbols are transmitted together with data symbols such that the receiver estimates the channel response from pilot symbols and compensates the received data symbols. Pilot-based channel estimation quality is limited by the number of pilot symbols and the received Signal-to-Noise Ratio (SNR). This paper presents performance of NB-IoT in the presence of channel estimation errors. In Section II we introduce the system model and derive analytical bound for the SNR gain from signal repetition. Practical NB-IoT uplink channel estimation algorithms and simulation results are presented in Section III. Section IV reports performance measurements from Software Defind Radio (SDR) based implementation of NB-IoT testbed. Finally, conclusion are drawn in Section V.

Notations: $\|\mathbf{v}\|$ and $\mathbf{v}^*$ denote Euclidean norm and complex conjugate of $\mathbf{v}$ respectively.

II. System Model

Let us consider the case where the same symbol, x, is repeatedly transmitted R times. The received signal is expressed as

$$\mathbf{y} = \mathbf{h}x + \mathbf{w} \tag{1}$$

where $\mathbf{y}, \mathbf{h}, \mathbf{w}$ are $R \times 1$ vectors of received signal, channel coefficient and Additive White Gaussian Noise (AWGN) respectively. For the sake of simplicity, we assume that $E\{|x|^2\} = 1$, $w_i \sim \mathcal{CN}(0,1)$, and $E\{\|\mathbf{h}[i]\|^2\} = \gamma$, $i = 0, \cdots, R-1$ such that the received SNR per symbol is γ. For ideal channel estimate $\hat{\mathbf{h}} = \mathbf{h}$. The received signals can be combined coherently yielding

$$\frac{\mathbf{h}^*}{\|\mathbf{h}\|}\mathbf{y} \quad = \|\mathbf{h}\|x + \tfrac{\mathbf{h}^*}{\|\mathbf{h}\|}\mathbf{w}. \tag{2}$$

Therefore, the effective SNR after coherent combing is $SNR_e = R\gamma$. This implies that with maximum repetition of NB-IoT physical channels (2048 for downlink and 128 for uplink), SNR gains of 33 dB and 21 dB receptively would be achieved. This suggests that a UE should be able to decode downlink channels even when the received signal is more than 25 dB below the noise floor. However, operation under such low signal level suffers even from small channel estimation error and hardware impairments such as clock drift and carrier frequency offset. One significant factor that should be considered is the channel estimation error. A non-ideal channel estimate, denoted by $\hat{\mathbf{h}}$, can be modeled as

$$\hat{\mathbf{h}} = \mathbf{h} + \mathbf{h}_e \tag{3}$$

$$\frac{\hat{\mathbf{h}}^*}{\|\hat{\mathbf{h}}\|} = \frac{\mathbf{h}^*}{\|\mathbf{h}\|} + \tilde{\mathbf{h}}_e \tag{4}$$

where $\mathbf{h}_e$ is the estimation error which has variance $E\{\|\mathbf{h}_e[i]\|^2\} = \sigma$. Assuming that $\mathbf{h}_e$ and $\mathbf{h}$ are independent, we get $E\{\|\hat{\mathbf{h}}[i]\|^2\} = \sigma + \gamma$.

$$\frac{\hat{\mathbf{h}}^*}{\|\hat{\mathbf{h}}\|}\mathbf{y} \quad = \tfrac{\|\mathbf{h}\|^2}{\|\mathbf{h}+\mathbf{h}_e\|}x + \tfrac{\mathbf{h}_e^*\mathbf{h}}{\|\mathbf{h}+\mathbf{h}_e\|}x + \tilde{\mathbf{w}} \tag{5}$$

where $\tilde{\mathbf{w}} = (\hat{\mathbf{h}}^*/\|\hat{\mathbf{h}}\|)\mathbf{w}$ is the Gaussian noise with unit variance.

$$E\{\|\tilde{\mathbf{w}}\|^2\} = 1 \tag{6}$$

From equation (5), the average signal power can be approximated as

$$E\left\{\frac{\|\mathbf{h}\|^4}{\|\mathbf{h}+\mathbf{h}_e\|^2}\right\} \approx \frac{1}{E\{1/\|\mathbf{h}\|^2\} + E\{\|\mathbf{h}_e\|^2/\|\mathbf{h}\|^4\}} \tag{7}$$

$$\approx \frac{R\gamma}{1+\sigma/2\gamma}. \tag{8}$$

Similarly,

$$E\left\{\frac{\|\mathbf{h}_e^*\mathbf{h}\|^2}{\|\mathbf{h}+\mathbf{h}_e\|^2}\right\} \approx \frac{E\{\|\mathbf{h}_e^*\mathbf{h}\|^2\}}{E\{\|\mathbf{h}+\mathbf{h}_e\|^2\}} = \frac{\sigma\gamma}{\sigma+\gamma}. \tag{9}$$

Therefore, the approximated effective SNR becomes

$$SNR_e \approx \frac{R(\sigma+\gamma)}{(\sigma+1+\sigma/\gamma)(1+\sigma/2\gamma)}. \tag{10}$$

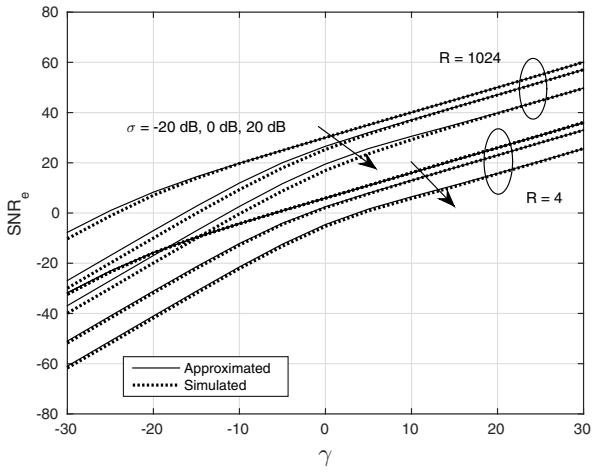

Fig. 2. SNR after coherent combining.

Fig. 2 shows that the approximated SNR_e is closely following the simulated values. SNR_e is impacted by both received SNR, γ, and channel estimation error, σ. The later one depends on the environment and channel estimation method. NB-IoT uses training pilot symbols for channel estimation. The number of training pilot symbols determines the channel estimation quality. Moreover, γ and σ are interdependent. As γ decreases, amplitude of the received pilot symbols decreases thereby increasing the estimation error σ. NB-IoT is expected to provide improved coverage by repeatedly transmitting the same data over multiple slots. Hence, the typical operating SNR is likely to be $\ll 0$ dB which suggests that channel estimation error is significant. In the following section, we analyze channel estimation problem in uplink data transmission.

III. Uplink Channel Estimation for NB-IoT

The UE transmits its data over narrow-band Physical Uplink Shared Channel (PUSCH) called NB-PUSCH. As illustrated in Fig. 3, resource grid structure of NB-PUSCH resembles LTE's PUSCH with normal cyclic prefix duration. In every slot, sub-carriers of the fourth OFDM symbol carry pilot symbols. For 15 kHz sub-carrier spacing, there are 12 pilot symbols per slot where there are two slots in a subframe. The channel estimation process can be split into two phases. First, pilot symbols are used to estimate channel response on sub-carriers which carry pilot symbols. This can be done by using, for example, Zero-Forcing (ZF) estimator or Minimum Mean Squared Error (MMSE) estimator. From this, we get channel estimates for all sub-carriers of OFDM symbols $l = 3, 10$. Then, channel estimates for the rest of OFDM symbols are computed using one-dimensional time-domain interpolation of the channel estimates of the two slots. In the following subsections, we compare commonly used channel estimators that can be used for NB-IoT.

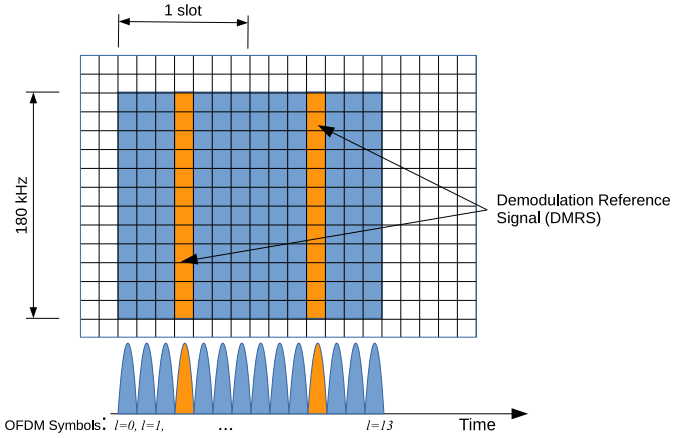

Fig. 3. Resource grid mapping of NB-PUSCH.

A. ZF Estimator

ZF is a simple pilot-based channel estimation method. It does not require prior information such as noise variance and statistics of the channel. Let the received pilot and data symbols for the k^{th} sub-carrier be

$$\mathbf{y}_p^{(k)} = \mathbf{h}^{(k)} s_k + \mathbf{w}_p^{(k)} \tag{11}$$

$$\mathbf{y}_d^{(k)} = \mathbf{h}^{(k)} d_k + \mathbf{w}_d^{(k)}, \quad k = 0, 2, \cdots, K-1 \tag{12}$$

respectively where s_k and d_k are pilot and data symbols transmitted on k^{th} sub-carrier, and $|s_k| = |d_k| = 1$. For each sub-carrier by which pilot symbols are transmitted, the ZF channel estimate is computed as a product of received symbol with conjugate of transmitted pilot symbol. Let us denote the channel response of k^{th} sub-carrier by $\mathbf{h}^{(k)}$. Hence,

$$\hat{\mathbf{h}}_{ZF}^{(k)} \triangleq s_k^* \mathbf{y}_p^{(k)} = \mathbf{h}^{(k)} + \mathbf{h}_e^{(k)}{}_{ZF} \tag{13}$$

where $\mathbf{h}_e^{(k)}{}_{ZF} = s_k^* \mathbf{w}_p^{(k)}$ is Gaussian-distributed estimation error with unit variance; $\sigma_{ZF}^2 = 1$.

B. MMSE Estimator

MMSE estimator exploits the knowledge of noise power and channel covariance matrix. For the Gaussian channel, we have

$$\hat{\mathbf{h}}_{MMSE}^{(k)} \triangleq \frac{\gamma}{1+\gamma} s_k^* \mathbf{y}_p^{(k)} = \frac{1}{1+1/\gamma} \hat{\mathbf{h}}_{ZF}^{(k)} \tag{14}$$

which is scaled version of ZF estimate. Since, NB-IoT uses Phase-Shift-Keying (PSK) modulation, the scaling factor has no impact on the receiver's performance. Moreover, accurate knowledge of channel covariance matrix is difficult to obtain in extremely low SNR situations.

C. Linear Phase (LP) Estimator

The LP estimator assumes a single-tap channel and low Doppler frequency such that frequency-domain channel response has constant amplitude and linear phase. This is because NB-IoT has narrow bandwidth (180 kHz), and UEs have low mobility. LP channel has the following form.

$$\mathbf{h}^{(k)} = \mathbf{D}\mathbf{h}^{(0)}, \quad k = 1, 2, \cdots, K-1 \tag{15}$$

$$\mathbf{D} \triangleq \begin{bmatrix} e^{jk\phi_0} & 0 & \cdots & 0 \\ 0 & e^{jk\phi_1} & & \vdots \\ \vdots & & \ddots & 0 \\ & \cdots & 0 & e^{jk\phi_{R-1}} \end{bmatrix}$$

where ϕ_i is the phase drift between consecutive sub-carriers of i^{th} repetition. We are now left with two unknown parameters: phase offset, $\mathbf{h}^{(0)}$, and slop of the channel phase response, ϕ. LP estimator computes these two parameters from ZF channel estimates. Consider channel estimate for the i^{th} repetition.

$$\mathbf{h}^{(k)}[i] = e^{jk\phi_i}\mathbf{h}^{(0)}[i] \tag{16}$$

Define

$$\Lambda_{i,m} \triangleq \frac{1}{K-m}\sum_{k=m}^{K-1} \hat{\mathbf{h}}_{ZF}^{(k)}[i]^* \hat{\mathbf{h}}_{ZF}^{(k-m)}[i] \tag{17}$$

$$= \|\mathbf{h}^{(0)}[i]\| e^{jm\phi_i} + \nu_{i,m} \tag{18}$$

where $\nu_{i,m}$ is zero-mean Gaussian noise with variance $(2\gamma + 1)/(K-m)$. Estimate for the phase drift, ϕ_i, can be computed from equation (18). Though multiple autocorrelations, $\Lambda_{i,m}$, with different lags, m, can be combined, phase ambiguity becomes a problem as m grows. Hence, we will use only $m = 1$ for phase drift estimation.

$$\hat{\phi}_i = \arg\{\Lambda_{i,1}\} \tag{19}$$

$$\hat{\mathbf{h}}^{(0)}[i] = \frac{1}{K}\sum_{k=0}^{K-1} \hat{\mathbf{h}}_{ZF}^{(k)}[i] e^{-jk\hat{\phi}_i} \tag{20}$$

Therefore, LP channel estimate becomes

$$\hat{\mathbf{h}}_{LP} = \hat{\mathbf{D}}\hat{\mathbf{h}}^{(0)} \tag{21}$$

where $\hat{\mathbf{D}} \triangleq \text{diag}\{e^{jk\hat{\phi}_0}, e^{jk\hat{\phi}_1}, \cdots, e^{jk\hat{\phi}_{R-1}}\}$.

D. Time-correlated channel

In our previous channel estimation analysis, we did not make any assumption regarding the time-correlation of channels. In real life situation, channel responses of consecutive symbols are correlated. Coherence time of the channel depends on the environment and on the mobility of the transmitter and/or the receiver. In many NB-IoT applications, the devices have little or no mobility. In this case, the surrounding environment is responsible for the channel fading. Prior knowledge of channel's time correlation can increase quality of channel estimates of individual symbols. This can be illustrated by considering the extreme scenario where the channel stays constant for all repetitions; $\mathbf{h}^{(k)} = \mathbf{1}_R h^{(k)}$ where $\mathbf{1}_R$ is $R \times 1$ vector of 1's.

$$\mathbf{y}_p^{(k)} = \mathbf{1}_R h^{(k)} s_k + \mathbf{w}_p^{(k)}, \quad k = 0, 2, \cdots, K-1 \tag{22}$$

Least Squares (LS) estimate of $h^{(k)}$ is

$$\hat{h}_{LS}^{(k)} = \frac{1}{R} s_k^* \mathbf{y}_p^{(k)} = h^{(k)} + \frac{1}{R} s_k^* \sum_i \mathbf{w}_p^{(k)}[i] \tag{23}$$

$$\hat{\mathbf{h}}_{LS} = \mathbf{h}^{(k)} + \mathbf{h}_e^{(k)}{}_{LS} \tag{24}$$

where $\mathbf{h}_e^{(k)}{}_{LS}[i] = \frac{1}{R}\sum_j \mathbf{h}_e^{(k)}{}_{ZF}[j]$ is zero-mean Gaussian distributed estimation error with variance $1/R$. This implies that channel estimation error is suppressed by a factor of R when all repetitions occur within the channel coherence time. In general, the number of repetitions that fall within the coherence time can be denoted as R_c where $R_c \leq R$ such that only R_c ZF channel estimates can be time-averaged. Without loss of generality, we can assume that $R = BR_c$ where B is the number of coherent channel blocks for which case the estimation error has variance $\sigma^2_{TA-ZF} = 1/R_c$. That is only rough estimation; correct estimation considers actual correlation between the repetitions and sums them with weights of correlation coefficients. The flat correlation approximation gives a lower bound on the performance. Time-averaged ZF (TA-ZF) channel estimate is given as

$$\hat{\mathbf{h}}_{TA-ZF}[i] = \frac{1}{R_c}\sum_{j=t_i}^{t_i+R_c-1} \hat{\mathbf{h}}_{ZF}[j] \tag{25}$$

where

$$t_i = \begin{cases} i, & i \leq R - R_c \\ R - R_c, & elsewhere \end{cases}.$$

Simulation results of the performance for the three channel estimators are shown in Fig. 4 and Fig. 5. Fig. 4 shows Bit Error Rate (BER) versus number of repetitions when the Doppler frequency is 80 Hz. We observe that LP performs better than ZF. Compared to ideal channel estimate, ZF and LP estimates have less gain for having more repetition. The SNR gain by increasing the repetition from 4 to 128 is only about 10 dB while in ideal case, 15 dB gain is achieved. TA-ZF performs slightly better than ZF and LP estimators. The gain is small as the channel coherent time is shorter. For lower Doppler frequency, TA-ZF has much better performance as shown in Fig. 5. This is due to the fact that the channel coherence time spans 32 consecutive symbols.

IV. Measurement

Besides analytical analysis and simulations, we have also implemented and measured physical layer performance of NB-IoT. This was done on SDR based NB-IoT testbed developed at Aalto University [11]. The testbed comprises standard desktop computer and Universal Software Radio Peripheral (USRP) [12] which are connected over Ethernet. The testbed implements physical layer and a subset of Medium Access Control (MAC) and Radio Resource Control (RRC) functionalities.

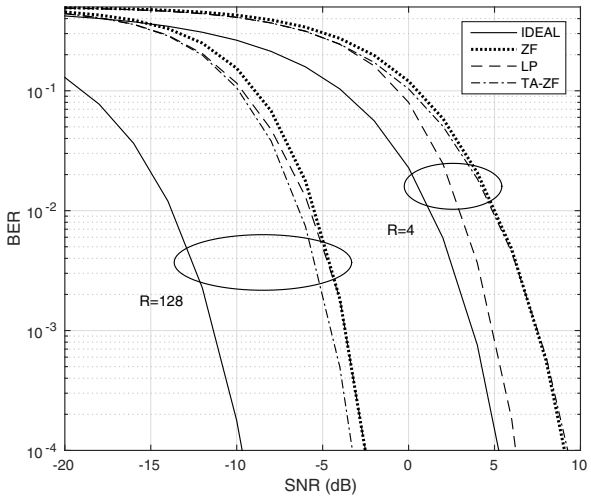

Fig. 4. Bit Error Rate for NB-IoT uplink shared channel with QPSK modulation and 15 kHz sub-carrier spacing. Doppler frequency $f_d = 80Hz$. This corresponds to $R_c = 2$ when one resource unit (subframe) is scheduled.

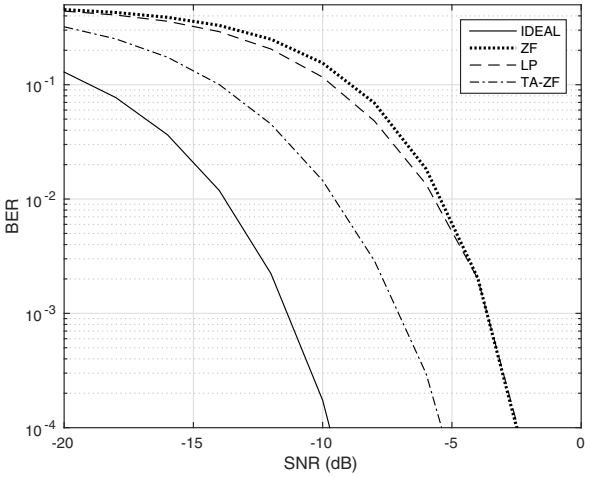

Fig. 5. Bit Error Rate for NB-IoT uplink shared channel with QPSK modulation and 15 kHz sub-carrier spacing. $R = 128$. Doppler frequency $f_d = 5.5Hz$. This corresponds to $R_c = 32$ when one resource unit (subframe) is scheduled.

All baseband processing and higher layer protocol stack are implemented in software using C++ programming language. The baseband I/Q samples are then transported over Ethernet to the USRP which upconverts and transmits them over the air. USRP X310 with UBX-160 daughterboard was used and can operate on any frequency band between 10 MHz to 6 GHz. During the measurement, the testbed was configured to operate on 640 MHz and 635 MHz carrier frequencies (we have license on these frequencies in our campus area) for downlink and uplink transmissions respectively. For the sake of measurement, in each transmission opportunity the Base Station (BS) schedules one UE. The BS allocates 2 uplink resource units with $R = 128$ maximum number of repetitions. The BS then attempts to decode NB-PUSCH data after every four repetition. In case of early successful decoding, the remaining uplink repetitions are discarded. The number of repetitions that are required to successfully decode the uplink data depends on the received SINR and the channel coherence time.

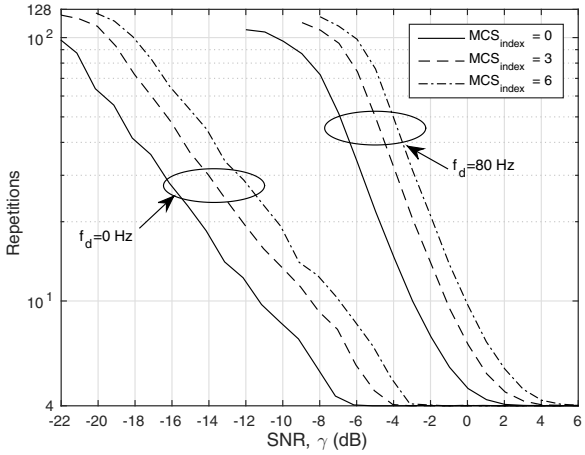

Fig. 6. Average number of repetitions required to decode NB-PUSCH transport block.

Measurements were carried out on both fast fading channel (Doppler frequency, $f_d = 80$ Hz) and static channel (Doppler frequency, $f_d = 0$ Hz). This allows us to see system performance variation between the two extremes. During the first measurement for a static channel ($f_d = 0$ Hz), the USRPs were fed from a common external 10 MHz reference clock and Pulse Per Second (PPS) trigger. This avoid unnecessary Doppler shift due to clock error. For the second measurement, an 80 Hz Doppler frequency was introduced into the channel. This make sure that signal repetitions fall outside coherence time of the channel. Moreover, external clock was not connected to the USRPs, and no Carrier Frequency Offset (CFO) compensation was applied at the receiver. According to [13], the internal clock of USRP X310 has 2.5 part-per-million (ppm) accuracy.

Fig. 6 shows the average number of repetitions that were needed by the BS in order to successfully decode NB-PUSCH data. The plots show number of repetitions as a function of received SNR for different coding rates and Doppler frequencies. Packets that were lost are excluded in the statistics. Modulation and Coding Scheme (MCS) indices 0, 3 & 6 stand for TBS of 32, 104 & 176 bits respectively. The results show that performance gain from signal repetitions is limited by the channel coherence time. With 4 repetitions and the MCS index of 6, about 6 dB SNR is required for operations in fast fading channel. If the channel is static, however, the SNR can be as low as -2 dB. Similarly, when maximum repetitions and lowest MCS index are used, fast fading channel incurs more

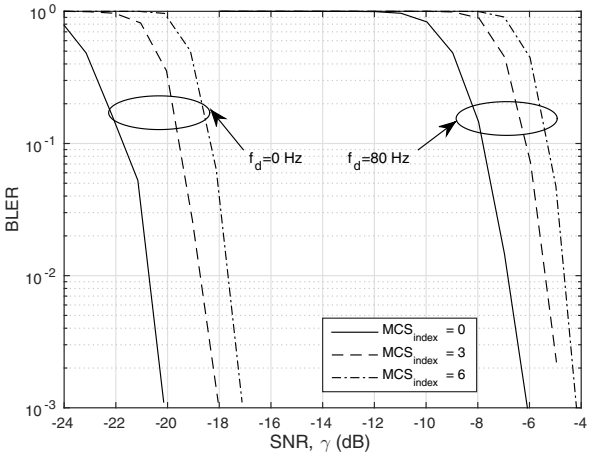

Fig. 7. Average Block Error Rate with maximum repetitions ($R = 128$).

than 10 dB coverage loss compared to the ideal static channel. Fig. 7 also confirms this claim. Fig. 7 shows the average Block Error Rate (BLER) when the BS schedules the UE to transmit with the maximum repetition ($R = 128$).

V. Conclusion

NB-IoT is a promising cellular technology for IoT applications. It can connect low-power IoT devices that are placed in weak coverage environments such as apartment basements. This is done be allowing devices to repeat signal transmissions while operating at very low power. Signal repetitions can boost the received signal quality. The performance gain is affected by the channel estimation quality which is limited by the channel coherent time. This paper presented uplink coverage performance analysis and simulation results for two extreme channel conditions. Moreover, the results were verified using real-life measurements for NB-IoT testebed implementation. It was observed that short channel coherence time significantly reduces the amount of coverage improvement that is expected from signal repetitions.

Acknowledgment

This work was partially supported by two projects that we would highly like to acknowledge their supports in here: (i) 5th Evolution Take of Wireless Communication Networks (TAKE-5), Finnish National 5G program funded by TEKES (Finnish National Foundation) and (ii) High Impact Initiative (HII) Advanced Connectivity Platform for Vertical Segment (ACTIVE) funded by EIT DIGITAL.

References

[1] Cellular networks for massive IoT-enabling low power wide area applications, white paper, 2016. Ericsson. [Online]. Available: {https://www.ericsson.com/res/docs/whitepapers/wp_iot.pdf}

[2] Visual Network Index (VNI) Complete Forecast Highlights, 2016. Cisco. [Online]. Available: {http://www.cisco.com/c/dam/m/en_us/solutions/service-provider/vni-forecast-highlights/pdf/Global_2020_Forecast_Highlights.pdf}

[3] J. Petäjäjärvi, K. Mikhaylov, M. Hämäläinen, and J. Iinatti, "Evaluation of LoRa LPWAN technology for remote health and wellbeing monitoring," in *2016 10th International Symposium on Medical Information and Communication Technology (ISMICT)*, March 2016, pp. 1–5.

[4] Sigfox. [Online]. Available: https://www.lora-alliance.org

[5] T. Adame, A. Bel, B. Bellalta, J. Barcelo, and M. Oliver, "IEEE 802.11AH: the WiFi approach for M2M communications," *IEEE Wireless Communications*, vol. 21, no. 6, pp. 144–152, December 2014.

[6] New Work Item: NarrowBand IOT (NB-IOT). TSG RAN Meeting #69, 2015. 3GPP. [Online]. Available: {www.3gpp.org/FTP/tsg_ran/TSG_RAN/TSGR_69/Docs/RP-151621.zip}

[7] New Study Item on Cellular System Support for Ultra Low Complexity and Low Throughput Internet of Things. TSG-GERAN Meeting #62, 2015. 3GPP. [Online]. Available: {http://www.3gpp.org/ftp/tsg_geran/TSG_GERAN/GERAN_62_Valencia/Docs/GP-140421.zip}

[8] TS 36.211 Evolved Universal Terrestrial Radio Access (E-UTRA) physical channels and modulation (Release 13), 2016. 3GPP. [Online]. Available: {http://www.3gpp.org/ftp/specs/archive/23_series/23.060/23060-3c0.zip}

[9] TS 36.213 Evolved Universal Terrestrial Radio Access (E-UTRA); Physical layer procedures (Release 13), 2016. 3GPP. [Online]. Available: {http://www.3gpp.org/ftp//Specs/archive/36_series/36.213/36213-d20.zip}

[10] TS 36.321 Evolved Universal Terrestrial Radio Access (E-UTRA); Medium Access Control (MAC) protocol specification (Release 13), 2016. 3GPP. [Online]. Available: {http://www.3gpp.org/ftp//Specs/archive/36_series/36.321/36321-d20.zip}

[11] Aalto University, "Researchers implemented a prototype for Narrowband Internet-of-Things system," *Press Release*, 28 June 2016. [Online]. Available: {http://elec.aalto.fi/en/current/news/2016-06-28/}

[12] Ettus research, August 2016. [Online]. Available: http://ettus.com

[13] USRP X300 and X310 Spec Sheet, 2016. Ettus Research. [Online]. Available: {https://www.ettus.com/content/files/X300_X310_Spec_Sheet.pdf}